International Journal of Applied Power Engineering (IJAPE)
Vol. 15, No. 1, March 2026, pp. 186~194
ISSN: 2252-8792, DOI: 10.11591/ijape.v15.i1.pp186-194

Modulation and performance analysis of two-wheeler electric vehicle

Debani Prasad Mishra[1], Rudranarayan Senapati[2], Pavan Kumar[1], Lakshay Bhardwaj[1], Surender Reddy Salkuti[3]
[1]Department of Electrical Engineering, IIIT Bhubaneswar, Odisha, India
[2]Department of Electrical Engineering, KIIT Deemed to be University, Odisha, India
[3]Department of Global Railways, Woosong University, Daejeon, Republic of Korea

Article Info

Article history:

Received Feb 13, 2024
Revised Nov 4, 2025
Accepted Nov 28, 2025

Keywords:

Battery management system
Drive cycle
Electric vehicles
MATLAB/Simulink
State of charge

ABSTRACT

When compared to traditional cars, electric vehicles (EVs) have less pollution, better fuel efficiency, and are better for the environment. This essay explores the evolution of EVs in great detail, emphasizing their vital role in lowering CO_2 emissions and promoting sustainability. It builds a dynamic model for EVs using MATLAB/Simulink, which explains the state of charge (SOC) and range prediction. The study emphasizes the importance of EVs in promoting a sustainable future by thoroughly covering design details, modeling, and a scientific methodology. Through the use of modeling to clarify technical aspects and highlight the significance of EV adoption, this study highlights the vital role that EVs play in reducing environmental impact and advancing environmentally friendly transportation. It highlights EVs' potential to revolutionize the automobile sector while promoting cleaner modes of transportation. It offers a thorough overview of EV production and usage and fervently promotes their wider acceptance as a means of laying the groundwork for a more sustainable and clean future.

Corresponding Author:

Surender Reddy Salkuti
Department of Global Railways, Woosong University
Jayang-Dong, Dong-Gu, Daejeon 34606, Republic of Korea
Email: surender@wsu.ac.kr

1. INTRODUCTION

There is expansion in the transportation industry almost everywhere in the world, and technological advancements and developments are also bringing about quick improvement. Electric vehicles (EVs) are being launched into the market because of this progress in the transportation sector. In this, the quick growth of a nation and an organization is reflected in the development and appearance of technology in all spheres of the modern world. A nation's ability to develop more quickly and easily is greatly influenced by its transportation system. Worldwide, the usage of fossil fuels has expanded, leading to a large increase in CO_2 emissions due to the strong demand for freight transportation in practically every industry15% of the world's CO_2 emissions come from the transportation sector [1], [2]. Twenty-five years after Thomas Parker invented the lead-acid battery, the first electric car was produced in 1884. Since then, a large number of electric cars have been released. Novas *et al*. [3] investigated the energy-related effects of various gearbox types. Additionally, a fixed gear system, a manual gearbox, and a CVT gearbox have all been used to study the powertrain system. Various types of electric cars (EVs), such as battery electric vehicles, plug-in hybrids, and fuel cells, were launched into the market to attain more power and torque, longer range on a single charge, and durability for the vehicle and motor vehicle. Battery electric vehicles are powered by electricity stored in

battery packs. Plug-in hybrids combine a gasoline or diesel engine with an electric motor and a large rechargeable battery [4], [5]. Fuel cell vehicles split electrons to produce electricity from hydrogen molecules to run the motor. Each of these EV models has benefits and drawbacks of its own. Nevertheless, because fossil fuels are expensive and conventional cars require expensive maintenance, there is a growing global demand for EVs, which is excellent news for the earth's ecosystem and its inhabitants. According to recent policy analyses, countries need coordinated policy frameworks to achieve climate targets, including large-scale electric vehicle adoption [6], [7]. By 2030, the worldwide share is predicted to rise from 2% in 2016 to 30% [8], [9]. By July 2022, the size of the worldwide EV market was $280 billion, and by 2026, it is projected to reach $1 trillion [10]. Northern markets, including those in America, Europe, and China, account for the majority of this increase. Electric vehicles with big-capacity batteries rely only on the onboard battery; all onboard electronics and electric motors run off separate batteries. Toxic contaminants are not released by electric vehicles, making them safe to drive. Consequently, electric cars will be seen as the most promising form of transportation soon. Batteries with a huge capacity power an electric vehicle. Batteries power a variety of onboard devices, including electric motors. One effective form of mobility in towns and villages is the automobile. The global fuel consumption of automobiles is rising dramatically. This accounts for almost half of the energy used in transportation worldwide. One of the biggest problems the world's ecology is currently confronting is energy conservation. As a result, there are numerous difficulties facing our global energy ecosystem. We believe that reducing future energy use will be significantly aided by transportation, even if every prediction about the future depends on energy. Over the past century, advances in internal combustion engine (ICE) technology have mostly focused on lowering pollutants and improving fuel efficiency [11], [12]. The main issues with EVs are battery-related, including their high starting costs, short driving ranges, and lengthy battery charging times [13].

An EV has been created through MATLAB simulation; it might be utilized to research the car model through the employment of formulae [14], [15]. The e-bike system's subsystems are simulated, and separate discussions are held for the battery (lithium-ion), controller (field direction control), motor (permanent magnet synchronous motor), range calculation, and status of the charge. To provide the required road responsiveness, the bicycle's dynamics have also been investigated and precisely modeled [16]. A lithium-ion (Li-ion) battery's power supply is a crucial part of the battery, and the MATLAB model relies on mathematical formulas. Every component is needed to create an EV system, as shown in Figure 1.

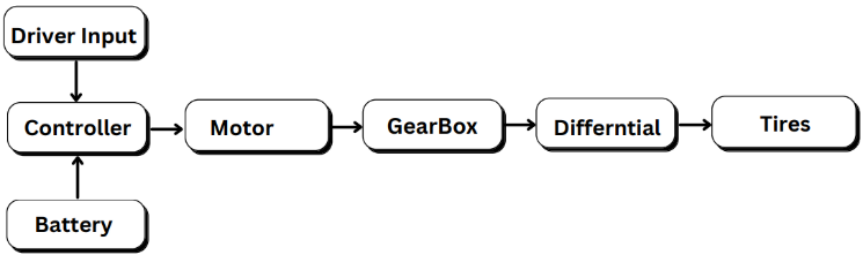

Figure 1. Block diagram for EV design

2. METHODOLOGY

The present generation of internal combustion engines will be rendered obsolete in automobiles due to factors such as excessive pollution levels, global warming, and approaching fuel shortages. Right now, the best car to drive is an electric one, because a wide range of expensive cars and modern technology are available to us. A lot of cars need to be registered and have certificates from the government. The seamless deployment of electric vehicles is hampered by numerous problems and restrictions. We suggest a two-wheeler in this model that doesn't need a car [17], [18]. According to government laws, helmets are not required when traveling by vehicle at speeds below 25 km/s per hour. This model is compatible with bicycles and scooters. This research suggests that small motor vehicles should be able to identify the places that use the most energy and suggest travel cycles [19]. The two-wheeler we are using's block layout is shown in Figure 2.

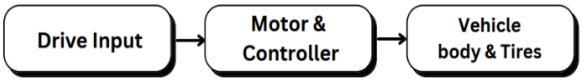

Figure 2. Electric vehicle body approach

2.1. The force of gravity and physics of flight

If two of the components are parallel to the motion and one is perpendicular to it, then no work is done in that direction. The equation will only take into account the parallel load component if the force is perpendicular [20].

$$Grav\ F = m \times g \times \sin(\alpha) \quad (1)$$

Where g stands for the gravitational constant, α is the angle created between the horizontal plane and the ground, and m is the two-wheel weight. The system's force, or aerodynamic flow, is what propels a scooter through a fluid (air).

$$F_{aero} = \frac{1}{2}\rho C_x S V^2 \quad (2)$$

Where ρ is 1.225 kg/m3, the air density. The drag coefficient, or C_x for this kind of car is roughly 0.9. The conductor surface is part of the front surface [21], [22], which is denoted by the letter S in m^2. V indicates how fast the scooter is moving relative to the air.

2.2. The force of rolling resistance and equilibrium of the forces

When motion is transmitted, power is lost through the wheels' contact with the ground. This loss is expressed in (3).

$$F_r = C_r \times m \times g \times cos(\alpha) \quad (3)$$

Where C_r is the rolling coefficient, which is equal to 0.1071; m is the system's total mass; g is gravity; and α is the slope's angle expressed in degrees. The mass of an item times its acceleration equals the sum of all forces acting on it, according to the first rule of motion [23]. Since each of the forces affecting the car has already been discussed, it is possible to determine its size. So that sufficient mechanical power must be given forth to make up for them. The (4) may be derived from (1)-(3), leading to (5).

$$M(\frac{dv}{dt}) = ft - f_{gra} - f_{aer} - f_r \quad (4)$$

$$P_{o/p} = (f_{ac} + f_{gra} + f_{aer} + f_v)V \quad (5)$$

3. DETAILS AND VALUES APPLIED TO THE EV DESIGN

Specific reference data under typical operating circumstances are needed for the design of electric vehicles. The TVS iQube standard and other simulation design factors have been taken into consideration in this investigation. This EV design's characteristics and parameters were all obtained from TVS's official website and the brochure files for each unique vehicle [24]. This simulation research has filtered all desired parameters. The parameters for the battery and motor, as well as all other characteristics affecting the vehicle, are listed in Tables 1 and 2, respectively. Permanent magnet synchronous motors (PMSMs) operating in three phases with a lithium-ion battery, and associated parts, are used in the TVS iQube EV.

In Table 1, a few of the TVS iQube Scooters system specifications that impact its effectiveness and performance are displayed in the table of contents. The overall body mass, frontal area, gear ratio, wheel size, and vehicle gradeability are among the characteristics [25], [26]. The weight of the scooter, including the battery and the rider, is the total body mass. When the scooter moves, the frontal area is the part that encounters air resistance. The gear ratio is the motor's speed divided by the wheel speed the tires' breadth and diameter equal the wheel sizes. The highest slope the scooter can climb without losing speed is known as vehicle gradability.

Table 2 illustrates some of the parameters that affect the TVS iQube electric scooter vehicle body and motion, and energy consumption is displayed in the table of contents. The air density, the rolling resistance force, the air drag force, the acceleration force, the angle of gradient, the coefficient of drag, and the rolling resistance coefficient are among the parameters [27], [28]. These variables control the force and resistance the scooters encounter when traveling at specific speeds and ground. The scooter performs and is more efficient the lower the resistance and the higher the force. As Table 3 shows, some of the lithium-ion battery parameters for the TVS iQube electric scooter are displayed in the table of contents [29]. The voltage, or the difference in electric potential between the battery's terminals; the capacity, or the maximum amount of energy the battery can hold; and the rated voltage, or the nominal voltage the battery can deliver, are all included in the battery specifications.

Table 1. Vehicle system specifications (taken from TVS official website)

Specifications	Principles
Total body mass (M)	117.8 kg
Frontal area (A)	0.7353 M^3
Gear ratio (G)	0.0097
Wheel size	90/90 - 12
Vehicle gradeability	0.12%

Table 2. Parameters acting on vehicle body (calculated)

Parameters	Values
Coefficient of drag (C_d)	0.15
Rolling resistance Coefficient (C_r)	0.5
Angle of gradient (α)	10^0
The air's density (ρ)	1.202 kg/m^3
Rolling resistance force (F_{rr})	12 N
Force of air drag (F_{dr})	96.19 N
Acceleration force (F_{ac})	256.5 N

Table 3. Battery specification (taken from TVS official website)

Parameters	Values
Voltage of battery	7.24 V
Capacity of battery	4.56 kWh
Rated voltage	52 V

4. EV DESIGNING APPROACHES IN SIMULINK

Six blocks are needed to build an EV system fully. Here, the simulation of all the blocks will be discussed step by step. In Figure 3, the driving cycle block is the first block diagram in the setup of the electric vehicle system. A header indicating the start of the design process with the driving cycle source will show on the Simulink file after starting and running the MATLAB/Simulink software [11]. This block acts as the beginning point for the design process, which may be accessed by going to the library browser and selecting the drive cycle block. Double-clicking on drive cycle will instantly reveal a selection of available drive cycles; if drive cycles are not already installed, add them. Drive cycle is essentially the most important block in the drive cycle source configuration [30], [31]. A range of external source formats, including Excel files, sliders, data sheets, and so on, can also be used to add a new drive cycle source to the library.

Figure 4 illustrates the design of driver control. In this control, the longitudinal driver block is currently powered by a driver controller of the proportional-integral (PI) type. It features three ports for input and three for output. This uses the VelFdbk port to provide feedback to the PI controller and the VelRef port as input for the drive cycle. Additionally, the controlled voltage source receives the acceleration command signal and forwards it to the H-bridge's connected regulated pulse width modulation (PWM) voltage block. In the design of the motor controller, as shown in Figure 5, EV is a key tool for motor vehicle operation. Therefore, motor control is used for proper vehicle handling and efficient regenerative braking. During deceleration, the library's H-bridge converter is taken out in order to control the engine and generate fresh power [12]. The brake input port, the reference, and the PWM input port are all electrically grounded. The driver controller's signal is connected to the PWM output of the regulated PWM voltage block. The motor will be linked to both its positive and negative output terminals.

In the battery setup design, as shown in Figure 6, the battery setup has been designed after the motor controller design. A 7.24 V lithium-ion battery is anticipated. The battery has a 0.1-second response time, a 100% starting point of charge (SoC), and a rated capacity of 4.56 kWh. It has a current sensor that is wired to both the battery and the H-bridge. To document the state of charge (SoC) of the battery while it is being charged and discharged, a bus selector is connected to the battery. All that is needed to observe real-time data is to attach the display and scope to the selection block. Figure 7 displays the entire motor design configuration, although the motor's positive and negative terminals are linked to the H bridge and the stator is connected to a mechanical rotating reference, the motor's rotor is still coupled to the vehicle body's gear shaft [13]. To measure the torque, a torque sensor is positioned in the center.

The most fundamental, significant, and essential component of every vehicle is its body. A car's body is made up of several different sections; the most crucial being the frame, chassis, wheels, and power transmission components. Here, we'll start by choosing the car body from the Simulink library. Next, we will configure the vehicle body with all required specifications.

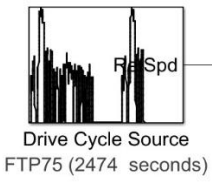

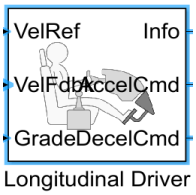

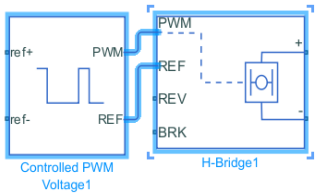

Figure 3. Set up for drive cycle source Figure 4. Driver control design Figure 5. Motor controller design

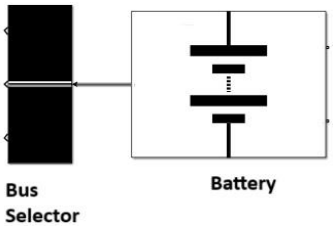

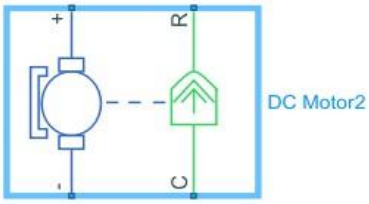

Figure 6. Battery setup and design Figure 7. DC motor setup design

5. BENCHMARK ELECTRICAL TWO-WHEELER MODEL

The body of the vehicle is attached to two tires with a hub and NR. The weight of an electric vehicle can be up to 600 kg. The drag coefficient is 0.5, and the frontal area is 2 m^2. Additionally, the differential is attached to the tires. We can optionally integrate additions and losses from viscous friction and gear machines with the aid of a differential. It links the DC motor and differential with the basic gear. The differential tire, on the other hand, joins the two axles. Using a scope to measure the vehicle's actual speed and a PS-Simulink converter to display the digital number, the display shows the speed. On one side of the DC motor, there is a mechanical rotational reference and a basic gear; on the other, there is an electrical reference, an H-bridge, and a current sensor. A PWM voltage signal will be supplied by the control. The H bridge helps with braking, reversing, and acceleration, and we can manage both internal and external power supply in an H-bridge. To get an optimized model, we maintain the PWM amplitude at IV and the input threshold voltage at a very low value of 0.001, because the simulation is done in averaging mode to reduce the simulation time and make the output voltage 50 V. The master scaling of the PWM voltage input can be set to 1 for high values and 0 for low values. The longitudinal driver provides one or zero as the PWM's input. Connect the scope so you can see the motor's current, and the H-bridge to the electrical reference, where the solver, brake, and reverse are all connected. We refer to the additional subsystem in this system as the motor and controller. The control unit is changed to PI control, and the longitudinal driver's reference feedback unit is changed to km/h. However, the grade ability is set at a constant zero, and the maximum speed is limited to 100 km/h. The vehicle body provides feedback, while the signal builder provides the velocity reference. Acceleration and deceleration orders are derived from the feedback and sent to the PWM using the Simulink-PS converter in conjunction with the regulated voltage source.

6. RESULTS AND DISCUSSION

When evaluating the outcomes of the simulation, keep the following considerations in mind. In the results, our primary considerations are state of charge (SOC) and range estimation. It is evident from the SOC findings that the battery discharges nonlinearly for the first 100 seconds and then linearly for the next 100. In addition, feedback allows it to be charged and drained in 200 seconds. Time is displayed on the x-axis for both curves, while the voltage and speed are depicted on the y-axis, respectively. From which the real speed and the reference speed are derived. The primary finding from the data is that the average speed is roughly 50 km/h. The battery has a voltage of 52 V, and it is evident that the real speed matches the reference speed [15], [16]. Depending on the given driving signal, the maximum speed in practice may not reach the reference maximum speed, but it is still getting close to the reference value. The car is reaching a range of 5.632 km during an average drive cycle, and its state of charge is still 76.07%. Figures 8 and 9 demonstrate how the torque increases along with acceleration, and how the battery charge decreases as acceleration increases. But the battery charge is increasing while the acceleration is decreasing, which means that the regenerative braking is working as shown in the picture.

Figure 10 illustrates a trend of increasing current over time by plotting the current in amperes against time in seconds. Figure 11, on the other hand, shows the voltage in volts plotted against time in seconds, showing that the voltage remained constant at 8 volts throughout the duration. A progressive increase in current from 200 A to 1000 A during the specified time interval is seen in Figure 10's current versus time graph. This shows that the current and time have a positive association, meaning that the current increases steadily with time. Conversely, Figure 11 shows the voltage versus time graph, which shows 8 V as a steady voltage level for the whole-time interval. A steady and unchanging voltage supply is shown by this consistent voltage reading, which implies that the voltage stays constant and does not change over time.

Describe the vehicle body's speed and the drive cycle's speed about time in Figure 12. The vehicle body speed is indicated by the blue line graph, and the derivative cycle body speed v/s time is indicated by the red line. This study compares the vehicle's performance with a specified drive cycle to assess the vehicle's efficiency. Here, the car is given the FTP75 (2474 sec) drive cycle. The yellow line shows the speed of the automobile after the drive cycle, while the blue line represents the drive cycle.

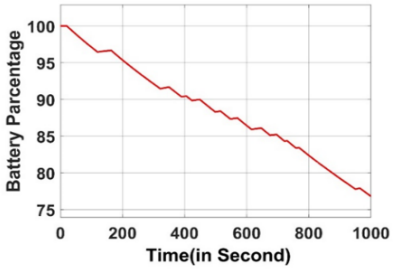

Figure 8. Battery state of charge vs time

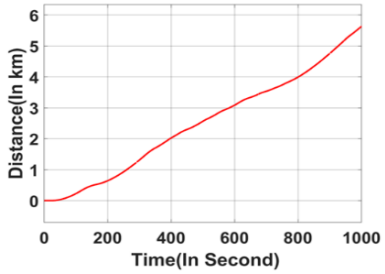

Figure 9. Distance travelled vs time

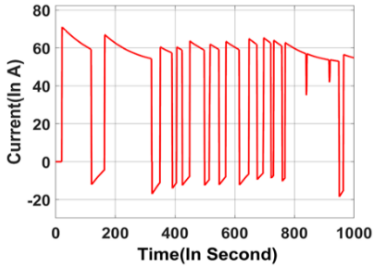

Figure 10. Current vs time

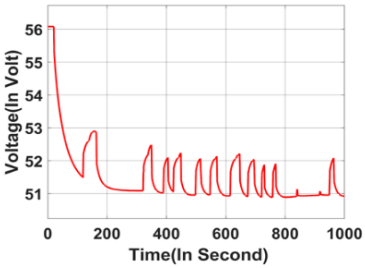

Figure 11. Voltage vs time

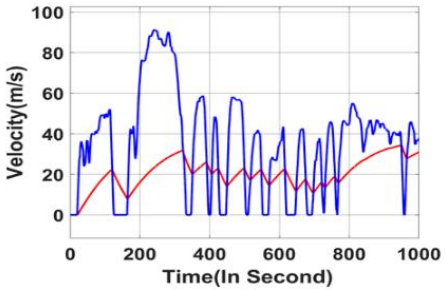

Figure 12. Speed of the vehicle and drive cycle vs time

7. CONCLUSION

In this paper, a simulation of a 2-wheeler electric vehicle has been carried out using MATLAB/Simulink, and a thorough, step-by-step method for designing an electric vehicle has been covered. Studies have also been done on SOC, range estimation, and speed. The battery voltage is limited to an average of 48 V. Studies also reveal that the model can be improved by utilizing the many drive cycles that are accessible and BLDC motors, which are widely employed in modern EV for it, to preserve energy. This study provides a step-by-step way to help researchers, students, and beginners in this sector use MATLAB/Simulink tools for EV designing and performance analysis.

FUNDING INFORMATION

This research work was supported by "Woosong University's Academic Research Funding - 2025".

AUTHOR CONTRIBUTIONS STATEMENT

This journal uses the Contributor Roles Taxonomy (CRediT) to recognize individual author contributions, reduce authorship disputes, and facilitate collaboration.

Name of Author	C	M	So	Va	Fo	I	R	D	O	E	Vi	Su	P	Fu
Debani Prasad Mishra	✓	✓		✓	✓	✓				✓		✓	✓	
Rudranarayan Senapati	✓			✓	✓					✓		✓	✓	
Pavan Kumar		✓	✓		✓	✓			✓	✓	✓			✓
Lakshay Bhardwaj		✓	✓		✓	✓			✓		✓			
Surender Reddy Salkuti	✓			✓		✓				✓		✓	✓	✓

C : **C**onceptualization
M : **M**ethodology
So : **So**ftware
Va : **Va**lidation
Fo : **Fo**rmal analysis
I : **I**nvestigation
R : **R**esources
D : **D**ata Curation
O : Writing - **O**riginal Draft
E : Writing - Review & **E**diting
Vi : **Vi**sualization
Su : **Su**pervision
P : **P**roject administration
Fu : **Fu**nding acquisition

CONFLICT OF INTEREST STATEMENT

Authors state no conflict of interest.

DATA AVAILABILITY

The datasets used and/or analyzed during the current study are available from the corresponding author on reasonable requests.

REFERENCES

[1] K. Tánczos and Á. Török, "Impact of transportation on environment," *Periodica Polytechnica Transportation Engineering*, vol. 36, no. 1–2, pp. 105–110, 2008, doi: 10.3311/pp.tr.2008-1-2.19.

[2] V. Simic, I. Gokasar, M. Deveci, and L. Švadlenka, "Mitigating climate change effects of urban transportation using a type-2 neutrosophic MEREC-MARCOS model," *IEEE Transactions on Engineering Management*, vol. 71, pp. 3233–3249, 2024, doi: 10.1109/TEM.2022.3207375.

[3] N. Novas *et al.*, "Global perspectives on and research challenges for electric vehicles," *Vehicles*, Nov. 2022, doi: 10.3390/vehicles4040066.

[4] A. A. Ismail, N. T. Mbungu, A. Elnady, R. C. Bansal, A.-K. Hamid, and M. AlShabi, "Impact of electric vehicles on smart grid and future predictions: a survey," *International Journal of Modelling and Simulation*, vol. 43, no. 6, pp. 1041–1057, Nov. 2023, doi: 10.1080/02286203.2022.2148180.

[5] J. A. Sanguesa, V. Torres-Sanz, P. Garrido, F. J. Martinez, and J. M. Marquez-Barja, "A review on electric vehicles: technologies and challenges," *Smart Cities*, vol. 4, no. 1, pp. 372–404, Mar. 2021, doi: 10.3390/smartcities4010022.

[6] International Energy Agency, Global EV Outlook 2024. IEA, Paris, 2024. [Online]. Available: https://www.iea.org/reports/global-ev-outlook-2024.

[7] International Energy Agency, Net Zero by 2050: a roadmap for the global energy sector. IEA, Paris, 2021. [Online]. Available: https://www.iea.org/reports/net-zero-by-2050.

[8] A. Guizani, M. Hammadi, J.-Y. Choley, T. Soriano, M. S. Abbes, and M. Haddar, "Electric vehicle design, modelling and optimization," *Mechanics & Industry*, vol. 17, no. 4, p. 405, Mar. 2016, doi: 10.1051/meca/2015095.

[9] Z. Chen, R. Xiong, and J. Cao, "Particle swarm optimization-based optimal power management of plug-in hybrid electric vehicles considering uncertain driving conditions," *Energy*, vol. 96, pp. 197–208, Feb. 2016, doi: 10.1016/j.energy.2015.12.071.

[10] G. Thejasree and R. Maniyeri, "E-bike system modeling and simulation," in *2019 IEEE International Conference on Intelligent Systems and Green Technology (ICISGT)*, Jun. 2019, pp. 9–95, doi: 10.1109/ICISGT44072.2019.00017.

[11] D. K. Kohar, A. K. Pati, and S. Nanda, "Design approaches and performance analysis of electric vehicle using MATLAB/Simulink," in *2023 IEEE International Students' Conference on Electrical, Electronics and Computer Science (SCEECS)*, Feb. 2023, pp. 1–6, doi: 10.1109/SCEECS57921.2023.10063009.

[12] M. T. P., G. A. M. P, and A. K. Parvathy, "Development of electric vehicle model in MATLAB/Simulink," in *2022 8th International Conference on Smart Structures and Systems (ICSSS)*, Apr. 2022, pp. 01–07, doi: 10.1109/ICSSS54381.2022.9782171.

[13] A. Mohanty, P. V. Manitha, and S. Lekshmi, "Simulation of electric vehicles using permanent magnet DC motor," in *2022 4th International Conference on Smart Systems and Inventive Technology (ICSSIT)*, Jan. 2022, pp. 1020–1025, doi: 10.1109/ICSSIT53264.2022.9716549.

[14] M. A. Djeziri, R. Merzouki, B. O. Bouamama, and M. Ouladsine, "Fault diagnosis and fault-tolerant control of an electric vehicle overactuated," *IEEE Transactions on Vehicular Technology*, vol. 62, no. 3, pp. 986–994, Mar. 2013, doi: 10.1109/TVT.2012.2231950.

[15] R. Yang, R. Xiong, and W. Shen, "On-board soft short circuit fault diagnosis of lithium-ion battery packs for electric vehicles using extended Kalman filter," *CSEE Journal of Power and Energy Systems*, vol. 8, no. 1, pp. 258–270, 2020, doi: 10.17775/CSEEJPES.2020.03260.

[16] K. Zhang *et al.*, "An early soft internal short-circuit fault diagnosis method for lithium-ion battery packs in electric vehicles," *IEEE/ASME Transactions on Mechatronics*, vol. 28, no. 2, pp. 644–655, Apr. 2023, doi: 10.1109/TMECH.2023.3234770.
[17] A. K. Mohanty, P. S. Babu, and S. R. Salkuti, "Fuzzy-based simultaneous optimal placement of electric vehicle charging stations, distributed generators, and DSTATCOM in a distribution system," *Energies*, vol. 15, no. 22, p. 8702, Nov. 2022, doi: 10.3390/en15228702.
[18] M. A. Hannan, M. M. Hoque, A. Hussain, Y. Yusof, and P. J. Ker, "State-of-the-art and energy management system of lithium-ion batteries in electric vehicle applications: issues and recommendations," *IEEE Access*, vol. 6, pp. 19362–19378, 2018, doi: 10.1109/ACCESS.2018.2817655.
[19] S. Aouaouda, M. Chadli, and M. Boukhnifer, "Speed sensor fault tolerant controller design for induction motor drive in EV," *Neurocomputing*, vol. 214, pp. 32–43, 2016, doi: 10.1016/j.neucom.2016.06.001.
[20] W. Lang, Y. Hu, C. Gong, X. Zhang, H. Xu, and J. Deng, "Artificial intelligence-based technique for fault detection and diagnosis of EV motors: A review," *IEEE Transactions on Transportation Electrification*, vol. 8, no. 1, pp. 384–406, Mar. 2022, doi: 10.1109/TTE.2021.3110318.
[21] K. Yatsugi, S. E. Pandarakone, Y. Mizuno, and H. Nakamura, "Common diagnosis approach to three-class induction motor faults using stator current feature and support vector machine," *IEEE Access*, vol. 11, pp. 24945–24952, 2023, doi: 10.1109/ACCESS.2023.3254914.
[22] J. S. Hsu, "Monitoring of defects in induction motors through air-gap torque observation," *IEEE Transactions on Industry Applications*, vol. 31, no. 5, pp. 1016–1021, 1995, doi: 10.1109/28.464514.
[23] J. A. Corral-Hernandez and J. A. Antonino-Daviu, "Thorough validation of a rotor fault diagnosis methodology in laboratory and field soft-started induction motors," *Chinese Journal of Electrical Engineering*, vol. 4, no. 3, pp. 66–72, Sep. 2018, doi: 10.23919/CJEE.2018.8471291.
[24] M. Z. Ali, M. N. S. K. Shabbir, S. M. K. Zaman, and X. Liang, "Machine learning based fault diagnosis for single-and multi-faults for induction motors fed by variable frequency drives," in *2019 IEEE Industry Applications Society Annual Meeting*, Sep. 2019, pp. 1–14, doi: 10.1109/IAS.2019.8912395.
[25] G. Liu, M. Zhao, Q. Chen, W. Zhao, and X. Zhu, "Performance comparison of fault-tolerant control for triple redundant 3 × 3-phase motors driven by mono-inverter," *IEEE Transactions on Transportation Electrification*, vol. 8, no. 2, pp. 1839–1852, Jun. 2022, doi: 10.1109/TTE.2021.3115482.
[26] S. R. Salkuti, "Advanced technologies for energy storage and electric vehicles," *Energies*, vol. 16, no. 5, p. 2312, Feb. 2023, doi: 10.3390/en16052312.
[27] A. Stief, J. R. Ottewill, J. Baranowski, and M. Orkisz, "A PCA and two-stage Bayesian sensor fusion approach for diagnosing electrical and mechanical faults in induction motors," *IEEE Transactions on Industrial Electronics*, vol. 66, no. 12, pp. 9510–9520, Dec. 2019, doi: 10.1109/TIE.2019.2891453.
[28] M. N. S. K. Shabbir, X. Liang, and S. Chakrabarti, "An ANOVA-based fault diagnosis approach for variable frequency drive-fed induction motors," *IEEE Transactions on Energy Conversion*, vol. 36, no. 1, pp. 500–512, Mar. 2021, doi: 10.1109/TEC.2020.3003838.
[29] J. S. L. Senanayaka, H. Van Khang, and K. G. Robbersmyr, "Multiple classifiers and data fusion for robust diagnosis of gearbox mixed faults," *IEEE Transactions on Industrial Informatics*, vol. 15, no. 8, pp. 4569–4579, Aug. 2019, doi: 10.1109/TII.2018.2883357.
[30] S. Pagidipala and S. Vuddanti, "Solving realistic reactive power market clearing problem of wind-thermal power system with system security," *International Journal of Emerging Electric Power Systems*, vol. 23, no. 2, pp. 125–144, Apr. 2022, doi: 10.1515/ijeeps-2021-0060.
[31] S. R. Salkuti, "Modeling of various renewable energy resources for smart electrical power systems," in *Next Generation Smart Grids: Modeling, Control and Optimization*, 2022, doi: 10.1007/978-981-16-7794-6_2.

BIOGRAPHIES OF AUTHORS

Debani Prasad Mishra is currently serves as an assistant professor and the head of the Electrical Engineering Department at the International Institute of Information Technology, Bhubaneswar, Odisha. He completed his bachelor's degree in electrical engineering from Biju Patnaik University of Technology, Odisha, in 2006, followed by a master's degree in power systems from IIT Delhi, India, in 2010. In 2019, he successfully obtained his Ph.D. in power systems from Veer Surendra Sai University of Technology, Odisha, India. With a profound academic background and extensive knowledge of power systems, he actively engages in teaching and research activities. He is deeply passionate about sharing his expertise and guiding aspiring students in the captivating field of electrical engineering. He can be contacted at email: debani@iiit-bh.ac.in.

Rudranarayan Senapati received the B.Tech. in electrical engineering from Utkal University, Odisha, India, in 2001 and the M.Tech. in communication system engineering in 2008 from KIIT University, Odisha. He has been awarded a Ph.D. degree in electrical engineering from KIIT deemed to be University, Patia Bhubaneswar, Odisha, India, in 2018. He is currently serving as an assistant professor in the School of Electrical Engineering, KIIT, deemed to be University, Patia, Bhubaneswar, Odisha. His research interests include solar forecasting, blockchain technology, renewable integration to power systems, and power quality. He can be contacted at email: rsenapatifel@kiit.ac.in.

Pavan Kumar is currently pursuing a B.Tech. degree in electrical and electronics engineering at the International Institute of Information Technology, Bhubaneswar, Odisha, India (batch 2021-2025). His interesting domains are web development, artificial intelligence, power electronics, electric drives, and electric vehicles. He can be contacted at email: b321055@iiit-bh.ac.in.

Lakshay Bhardwaj is currently pursuing a B.Tech. degree in electrical and electronics engineering at the International Institute of Information Technology, Bhubaneswar, Odisha, India (batch 2021-2025). His areas of interest are web development, artificial intelligence, power electronics, and advancements in EV battery technology exploration. He can be contacted at email: b321061@iiit-bh.ac.in.

Surender Reddy Salkuti received a Ph.D. degree in electrical engineering from the Indian Institute of Technology, New Delhi, India, in 2013. He was a postdoctoral researcher at Howard University, Washington, DC, USA, from 2013 to 2014. He is currently an associate professor at the Department of Railroad and Electrical Engineering, Woosong University, Daejeon, Republic of Korea. His current research interests include market clearing, including renewable energy sources, demand response, and smart grid development with integration of wind and solar photovoltaic energy sources. He can be contacted at email: surender@wsu.ac.kr.